Hindawi Publishing Corporation
Journal of Chemistry
Volume 2013, Article ID 959761, 8 pages
http://dx.doi.org/10.1155/2013/959761

Research Article

Breakthrough Curve Analysis for Column Dynamics Sorption of Mn(II) Ions from Wastewater by Using *Mangostana garcinia* Peel-Based Granular-Activated Carbon

Z. Z. Chowdhury,[1] S. M. Zain,[1] A. K. Rashid,[1] R. F. Rafique,[2] and K. Khalid[3]

[1] *Department of Chemistry, Faculty of Science, University Malaya, 50603 Kuala Lumpur, Malaysia*
[2] *Department of Environmental Engineering, Faculty of Engineering, Yangho-dong, Gumi, Gyeongbuk 730-701, Republic of Korea*
[3] *Malaysian Agricultural Research and Development Institute (MARDI), 43400 Serdang, Malaysia*

Correspondence should be addressed to Z. Z. Chowdhury; zaira.chowdhury76@gmail.com

Received 10 March 2012; Accepted 19 April 2012

Academic Editor: Dimosthenis L. Giokas

Copyright © 2013 Z. Z. Chowdhury et al. This is an open access article distributed under the Creative Commons Attribution License, which permits unrestricted use, distribution, and reproduction in any medium, provided the original work is properly cited.

The potential of granular-activated carbon (GAC) derived from agrowaste of Mangostene (*Mangostana garcinia*) fruit peel was investigated in batch and fixed bed system as a replacement of current expensive methods for treating wastewater contaminated by manganese, Mn(II) cations. Batch equilibrium data was analyzed by Langmuir, Freundlich, and Temkin isotherm models at different temperatures. The effect of inlet metal ion concentration (50 mg/L, 70 mg/L, and 100 mg/L), feed flow rate (1 mL/min and 3 mL/min), and activated carbon bed height (4.5 cm and 3 cm) on the breakthrough characteristics of the fixed bed sorption system were determined. The adsorption data were fitted with well-established column models, namely, Thomas, Yoon-Nelson, and Adams-Bohart. The results were best-fitted with Thomas and Yoon-Nelson models rather than Adams-Bohart model for all conditions. The column had been regenerated and reused consecutively for five cycles. The results demonstrated that the prepared activated carbon was suitable for removal of Mn(II) ions from wastewater using batch as well as fixed bed sorption system.

1. Introduction

Among various pollutants present in surface water, inorganic species of heavy metals and their metalloids are of major concern as they are difficult to remove owing to their smaller ionic size, complex state of existence, very low concentration in high volume, and competition with nontoxic inorganic species [1]. The presence of inorganic species especially divalent cations of manganese, Mn and its metalloids are commonly found in iron (Fe) bearing waste wastewater. The intake of manganese can cause neurological disorder in men when inhaled at concentration greater than >10 mg/day [1]. Even at lowest concentration, it produces objectionable stains on fabric [2–4]. Many industries, specially mining source discharge Mn(II) ions into natural freshwater bodies without sufficient prior treatment which is very difficult to remove as this is the last member of Irving William series which has least tendency to form stable surface complexes and thereby removed by sorption from wastewater.

Various technologies have been developed to address the deleterious effects of Mn(II) ions on the quality of fresh water, especially those emanating from mining sources. The most common approach to remove Mn(II) ions is to oxidize and subsequently precipitate it as MnO_2. However, this process of abiotic and biological oxidation is relatively slow at pH below 8 and is significantly inhibited by presence of iron (Fe) [2]. Partial removal of Mn(II) ions under reducing condition was reported to produce secondary pollutant of rhodochrosite ($MnCO_3$) [4]. Some previous studies reported to remove Mn(II) ions by using granular-activated carbon (41%), lignite (25.84%), and palm fruit bunch (50%) [5].

Adsorption onto commercial-activated carbon is an effective technique to remove heavy metals including manganese from waste effluents. Regardless of its extensive application in

wastewater treatment, commercial-activated carbon remains an expensive material. Coal, lignite, peat, and wood are frequently used for production of commercial activated carbon. However, production of activated carbon from these nonrenewable starting materials makes it costly [6, 7]. Therefore, the use of renewable source of low cost agricultural waste biomass which needs little processing to produce activated adsorbent is considered as a better choice [8, 9]. Hence aqueous phase adsorption by utilizing different types of agroresidues has gained credibility in recent years because of its excellent performance, biodegradability, and simplicity of design for treating waste effluents [10–12].

This study examines the performance of granular activated carbon prepared from agroresidues of Mangostene *(Mangostana garcinia)* fruit peel for adsorption of Mn(II) ion bearing wastewater in batch as well as fixed bed sorption system. Column dynamics has been investigated by using Thomas, Yoon-Nelson, and Adams-Bohart models. Nevertheless, column regeneration and recycling has been carried out until five cycles by considering the industrial applicability of the prepared sorbent.

2. Experimental

2.1. Preparation of Adsorbent. The fruit shells were first washed thoroughly to eliminate dust and inorganic matters on their surfaces. It was dried in an oven at temperature of 105°C for 24 h to remove all the moisture. The dried precursors were cut into small pieces and sieved to the size of 1.2 mm. 50 gm of dried fruit shell was placed on the metal mesh located at the bottom of the tubular reactor. Purified nitrogen gas was used to evacuate oxygen and create the inert atmosphere through the reactor. The flow rate of nitrogen gas and the heating, rate was maintained at 150 cm^3/min and 10°C/min, respectively. The temperature was increased from room temperature to 400°C and held for 2 h to produce char. The char was mixed up with KOH at ratio 1 : 1 and activated under CO_2 gas flow rate of 150 cm^3/min for 750°C at heating rate of 10°C/min. The prepared activated carbon was washed with hot deionized water for several times until the pH becomes 6-7, dried and stored in air tight container for further application.

2.2. Surface Characterization of the Adsorbent. Surface area, pore volume and pore size distribution of the raw precursor and prepared adsorbent was determined by using Autosorb-1, Quantachrome Autosorb Automated gas sorption system supplied by Quantachrome. Prepared activated carbon was outgassed under vacuum at temperature 300°C for 4 hours to remove any moisture content from the solid surface before performing the nitrogen gas adsorption. Surface area and pore volume were calculated by Brunauer Emmett Teller (BET). Above-mentioned procedure was automatically performed by software (Micropore version 2.26) which was supplied with the instrument.

Iodine number is one of the most essential parameters widely used to characterize the prepared activated carbon. 0.1 gm of activated carbon is placed with 25 mL of iodine solution in a 100 mL conical flask and was shaken for 1 minute. After that the solution was filtered and 10 mL of filtrate was taken inside a 100 mL conical flask. The solution is titrated with 0.04 N sodium thio-sulphate solutions until it becomes clear. The iodine number of the activated carbon was determined by using (1) which represents the number of milligrams of iodine adsorbed by one gram of activated carbon [13]:

$$\text{Iodine Number} = \frac{V x \left(T_i - T_f\right) x C_i x M_i}{T_i g}, \quad (1)$$

where V represents the volume of iodine solution (25 mL), T_i is the volume of Na_2SO_4 solution used for titration of 10 mL iodine solution, T_f is the volume of Na_2SO_4 solution used for titration of 10 mL of filtrate, g represents the weight of activated carbon (0.1 gm), M_i is the molar weight of Iodine (126.9044 g/mol), and C_i is the concentration of iodine solution (0.045 N) [13].

2.3. Batch Adsorption Study. The batch experiment was carried out by adding 0.2 gm of activated carbon with 50 mL of 50, 60, 70, 80, 90, and 100 mg/L solution of Mn(II) ions and shaking at agitation speed of about 150 rpm until the equilibrium contact time in water bath shaker at temperature 30°C, 50°C, and 70°C. The remaining concentration of the cations was analyzed after set interval of time until equilibrium by using atomic absorption spectrophotometer (PerkinElmer Model 3100). The amount of adsorption of Mn(II) ions at equilibrium, q_e (mg/g), was calculated by using the following (2) in batch sorption system:

$$q_e = \frac{\left(C_0 - C_e\right) V}{W}, \quad (2)$$

where q_e (mg/g) is the amount of ion adsorbed at equilibrium. C_0 and C_e (mg/L) are the liquid-phase concentrations of Mn(II) ions at initial and equilibrium conditions, respectively. V (L) is the volume of the solution, and W (g) is the mass of activated carbon used. The removal efficiency of the metal ion was calculated by dividing the residual metal ion concentration after equilibrium by initial metal ion concentration and the result is calculated on percentage basis.

2.4. Fixed Bed Adsorption Study. Figure 1 represents the schematic diagram of the fixed-bed adsorption system. Continuous flow adsorption studies were conducted in a column made of Pyrex glass tube having inner diameter of 4.5 cm and 25 cm height. A sieve made up of stainless steel was placed at the bottom of the column. Over the sieve, a layer of glass wool was placed to prevent loss of adsorbent. A peristaltic pump (Model Masterflex, Cole-Parmer Instrument Co., USA) was used to pump the feed upward through the column at a desired flow rate. The solution was pumped upward to avoid channeling due to gravity.

Column regeneration was carried out by using 1 M HNO_3 acid solution at flow rate 3 mL/min for 16 hours. After each cycle, the adsorbent was washed with hot distilled water and then packed inside the column. The regeneration efficiency

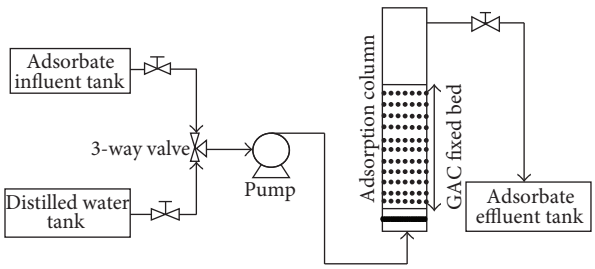

Figure 1: Schematic flow diagram of fixed bed system onto GAC.

(RE%) was calculated for bed height (4.5 cm), flow rate (1 mL/min), and initial concentration of 100 mg/L by using following (3):

$$\text{RE}\,(\%) = \frac{q_{\text{reg}}}{q_{\text{org}}} \times 100, \tag{3}$$

where q_{reg} is the adsorptive capacity of the regenerated column and q_{org} is the sorption capacity (mg/g) of the adsorbent after each cycle.

3. Results and Discussion

3.1. Surface Characterization of the Prepared Adsorbent. Surface area, pore volume, and pore size distribution of the prepared activated adsorbent is listed in Table 1. The raw fruit shell had BET surface area of 1.034 m^2/g, micro pore volume 0.0.0051 cc/g and pore diameter 4.087 Å. It was observed that, after the activation process, BET surface area and total pore volume increased significantly. This might be due to the reaction of both chemical and physical activating agents of KOH and CO_2 with the cellulosic precursor at high temperature during the activation process. Thus, it would increase the surface area by developing new pores inside the carbon matrix of the semicarbonized char [14]. Based on the International Union of Pure and Applied Chemistry (IUPAC 1972) classification, the pores can be categorized into three main types depending on pore diameters, such as micropores (pore size < 2 Å), mesopores (pore size 2–50 Å), and macro pores (pore size > 50 Å) [15]. Here, the activated carbon prepared had the average pore diameter of 28.9 Å which is in the range of mesoporous type of activated adsorbent [14].

3.2. Batch Adsorption Study. Batch equilibrium data obtained at 30°C–70°C were analyzed by using the linear form of Langmuir isotherm [16] equation which is expressed by (4):

$$\frac{C_e}{q_e} = \frac{1}{q_{\max} K_L} + \frac{C_e}{q_{\max}}, \tag{4}$$

where $q_{\max}$ (mg/g) is the maximum amount of the Mn(II) ions per unit weight of the activated carbon to form a complete monolayer on the surface whereas K_L (L/mg) is Langmuir constant related to the affinity of the binding sites.

Table 1: Surface characterization of the prepared adsorbent.

Physiochemical characteristics	Activated carbon
BET surface area	312.03 m^2/g
Total pore volume (DR method)	0.128 cm^3/g
Micropore surface area (DR method)	261.3 m^2/g
Average pore diameter	28.9 Å
Cumulative adsorption surface area (BJH method)	178.3 m^2/g
Iodine number	298.78 mg/g

The essential characteristics of the Langmuir equation can be expressed in terms of a separation factor, R_L which is given below:

$$R_L = \frac{1}{1 + K_L C_0}. \tag{5}$$

The linear form of Freundlich [17] isotherm is

$$\ln q_e = \ln K_F + \frac{1}{n} \ln C_e. \tag{6}$$

Here, K_F (mg/g) represents the affinity factor or multilayer adsorption capacity and $1/n$ is the intensity of adsorption, respectively.

According to Temkin isotherm [18], the linear form can be expressed by (7):

$$q_e = \frac{RT}{b} \ln K_T + \frac{RT}{b} \ln C_e. \tag{7}$$

Here, $RT/b = B$ (J/mol), which is Temkin constant related to heat of sorption, whereas K_T (L/g) represents the equilibrium binding constant corresponding to the maximum binding energy. R (8.314 J/mol K) is universal gas constant and T (°K) is absolute temperature. The model parameters at different temperature are listed in Table 2.

The results from Table 1 suggested the applicability of Langmuir model which reflected homogeneous texture of the prepared where adsorption of each cations of Mn(II) had equal activation energy. The R_L values obtained were less than 1 demonstrating that the adsorption of Mn(II) ions onto the prepared activated carbon is favorable. The positive value of K_F and the Freundlich exponent, $1/n$ ranging between 0 and 1, showed surface heterogeneity and favorable adsorption of Mn(II) ions onto the surface of prepared activated carbon [14]. The experimental data were further analyzed by Temkin isotherm which showed a higher regression coefficient, R^2 values, showing the linear dependence of heat of adsorption at low to medium coverage [14].

3.3. Fixed Bed Adsorption Study

3.3.1. Effect of Adsorbate Inlet Concentration. The effect of adsorbate Mn(II) ions concentration on the column performance was studied by varying the inlet concentration of 50, 70, and 100 mg/L for while the same adsorbent bed height

Table 2: Isotherm model parameters at different temperature.

Isotherm Model	Parameters	Temperature(°C)		
		30	50	70
Langmuir	q_m, Maximum monolayer adsorption capacities (mg/g)	24.39	27.02	28.57
	R_L, separation factor	0.118	0.097	0.094
	K_L, Langmuir constant	0.075	0.077	0.096
	R^2, correlation coefficient	0.965	0.949	0.962
Freundlich	K_F, affinity factor (mg/gm (L/mg)$^{1/n}$)	4.067	4.145	4.898
	$1/n$, Freundlich exponent	0.419	0.453	0.445
	R^2, correlation coefficient	0.918	0.937	0.951
Temkin	K_T, binding constant (L/mg)	1.056	0.6351	1.675
	B, Temkin constant	4.801	6.393	4.328
	R^2, correlation coefficient	0.937	0.935	0.972

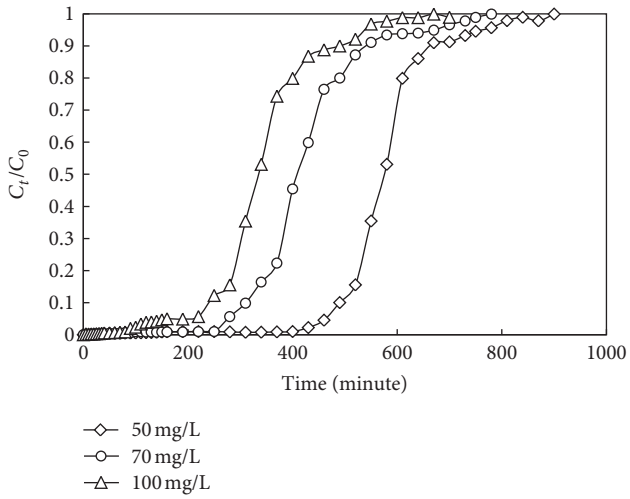

Figure 2: Breakthrough curves for adsorption of manganese (II) onto MFSAC for different Initial concentration (flow rate 1 mL/min, pH 5.5, temperature (30 ± 1°C)).

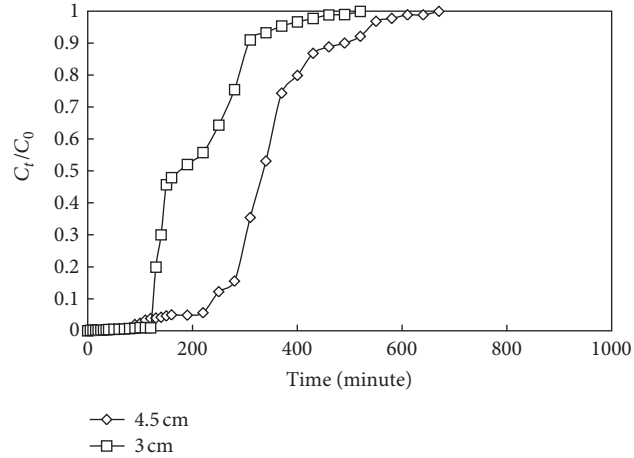

Figure 3: Breakthrough curves for adsorption of manganese(II) onto MFSAC for different Bed height (concentration 100 mg/L, flow rate 1 mL/min, pH 5.5, temperature (30 ± 1°C)).

of 4.5 cm and feed flow rate of 1 mL/min were used. The breakthrough curve is illustrated by Figure 2.

As can be observed from the plots (Figure 2), the activated carbon beds were exhausted faster at higher adsorbate inlet concentration that is, for 100 mg/L. That is earlier breakthrough point was reached at higher concentration. The breakpoint time was found to decrease with increasing adsorbate inlet concentration as the binding sites became more quickly saturated in the column. A decrease in inlet concentration gave an extended breakthrough curve, indicating that a higher volume of solution could be treated. This is due to the fact that lower concentration gradient caused a slower transport due to a decrease in diffusion coefficient or mass transfer coefficient [19, 20].

3.3.2. Effect of Activated Carbon Bed Height. Figure 3 shows the breakthrough curve obtained for adsorption of Mn(II) on MFSAC for two different bed height of 3 and 4.5 cm (3.56 and 4.86 g of MFSAC) at constant adsorbate feed flow rate of 1 mL/min and adsorbate inlet concentration of 100 mg/L.

As can be seen from the plots (Figure 3), both the break through time, t_b, and exhaustion time, t_e, were found to increase with increasing bed height. The plots represent that the shape and gradient of the breakthrough curves were slightly different with the variation of bed depth which is expected also. A higher uptake was observed at higher bed height due to the increase in the amount of the activated carbon which provided more fixations of the cations with active binding sites for the adsorption process to proceed. The increase in bed height will increase the mass transfer zone. The mass transfer zone in a column moves from the entrance of the bed and proceed towards the exit. Hence for same influent concentration and fixed bed system, an increase in bed height would create a longer distance for the mass transfer zone to reach the exit subsequently resulting an extended breakthrough time. For higher bed depth, the increase of adsorbent mass would provide a larger service area

leading to an increase in the volume of the treated solution [21].

3.3.3. Effect of Feed Flow Rate. The effect of feed flow rate on the adsorption of Mn(II) on MFSAC was investigate by varying the feed flow rate (1 and 3 mL/min) with constant adsorbent bed height of 4.5 cm and inlet adsorbate concentration of 100 mg/L, as shown by the breakthrough curve in Figure 4. The curve showed that at higher flow rate, the front of the adsorption zone quickly reached the top of the column that is the column was saturated early. Lower flow rate has resulted in longer contact time as well as shallow adsorption zone. At higher flow rate more steeper curve with relatively early breakthrough and exhaustion time resulted in less adsorption uptake.

3.4. Column Dynamics Study. The sorption performance of the cations through the column was analyzed by Thomas, Yoon-Nelson, and Adams-Bohart models starting at concentration ratio, $C_t/C_0 > 0.1$ that is 10% breakthrough until $C_t/C_0 > 0.90$, that is, 90% breakthrough for manganese by considering the safe water quality standards and operating limit of mass transfer zone of a column [21–23].

3.5. Application of the Thomas Model. Thomas model is based on the assumption that the process follows Langmuir kinetics of adsorption-desorption with no axial dispersion. It describes that the rate driving force obeys the 2nd order reversible reaction kinetics [24]. The linearized form of the model is given as:

$$\ln\left[\left(\frac{C_0}{C_t}\right)-1\right] = \left(\frac{k_{\mathrm{Th}}q_0 m}{Q}\right)-\left(\frac{k_{\mathrm{Th}}q_0 V_{\mathrm{eff}}}{Q}\right), \quad (8)$$

where k_{Th} (mL/mg min) is the Thomas rate constant q_0 (mg/g) is the equilibrium adsorbate uptake and m is the amount of adsorbent in the column.

The experimental data were fitted with Thomas model to determine the rate constant (k_{th}) and maximum capacity of sorption (q_0). The k_{th}, and q_0, values were calculated from slope and intercepts of linear plots of ln $[(C_0/C_t) - 1]$ against t using values from the column experiments (Figures not shown). From the regression coefficient (R^2) and other parameters, it can be concluded that the experimental data fitted well with Thomas model. The model parameters are listed in Table 3.

As the concentration increased, the value of k_{th} decreased whereas the value of q_0 showed a reverse trend, that is, increased with increase in concentration [19, 25]. The bed capacity (q_0) increased and the coefficient (k_{th}) increased with increase in bed height. Similarly, q_0 values decreased and k_{th} values increased with increase in the flow rate. Similar trend has also been observed for sorption of Cr(VI) by activated weed fixed bed column [26]. The well-fitting of the experimental data with the Thomas model indicate that the external and internal diffusion will not be the limiting step [19, 25].

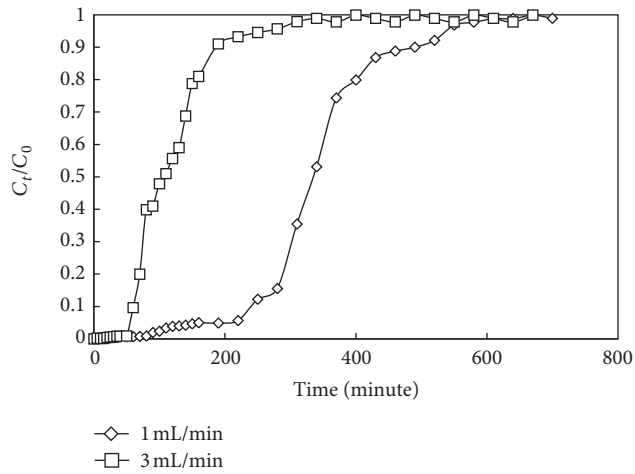

Figure 4: Breakthrough curves for adsorption of manganese(II) onto MFSAC for different flow rate (concentration 100 mg/L, pH 5.5, temperature (30 ± 1°C)).

3.6. Application of the Yoon-Nelson Model. A simple theoretical model developed by Yoon-Nelson was applied to investigate the breakthrough behavior of Mn(II) ions on MFS-based activated carbon. This model was derived based on the assumption that the rate of decrease in the probability of adsorption for each adsorbate molecule is proportional to the probability of adsorbate adsorption and the probability of adsorbate breakthrough on the adsorbent [27]. The linearized model for a single component system is expressed as:

$$\ln\left[\frac{C_t}{C_0 - C_t}\right] = k_{\mathrm{YN}}t - \tau k_{\mathrm{YN}}, \quad (9)$$

where k_{YN} (min^{-t}) is the rate constant and τ is the time required for 50% adsorbate breakthrough.

The values of K_{YN} and τ were estimated from slope and intercepts of the linear graph between $\ln[C_t/(C_0 - C_t)]$ versus t at different flow rates, bed heights, and initial cation concentration (figures are not shown). Values of K_{YN} was found to decrease with decrease in bed height whereas, the corresponding values of τ increased with increasing bed height. With increase in initial cation concentration, the K_{YN} and τ values decreased. With increase in flow rate, K_{YN} increased but τ decreased. Similar trend was flowed for sorption of azo dye and Cd(II) for column mode sorption [19, 21]. The values of K_{YN} and τ along with other statistical parameter are listed in Table 4.

3.7. Application of the Adams-Bohart Model. This model was established based on the surface reaction theory and it assumed that equilibrium is not instantaneous. Therefore the rate of adsorption was proportional to both the residual capacity of the activated carbon and the concentration of the sorbing species [28]. The mathematical equation of the model can be written as:

$$\mathrm{In}\left(\frac{C_t}{C_0}\right) = K_{\mathrm{AB}}C_{0t} - K_{\mathrm{AB}}N_0\left(\frac{z}{U_0}\right), \quad (10)$$

Table 3: Thomas model parameters for manganese (II) at different conditions using linear regression analysis.

Initial concentration (mg/L)	Bed height (cm)	Flow rate (mL/min)	k_{th} (mL/min-mg) × 10^{-4}	q_0 (mg/g)	R^2
50	4.5	1	5.20	6085.78	0.983
70	4.5	1	2.71	6162.33	0.975
100	4.5	1	1.70	7257.32	0.931
100	3.0	1	1.50	5574.90	0.890
100	4.5	3	2.80	6856.26	0.956

Table 4: Yoon-Nelson model parameters for manganese(II) at different conditions using linear regression analysis.

Initial Concentration (mg/L)	Bed Height (cm)	Flow Rate (mL/min)	K_{YN} (L/min)	ζ (min)	R^2
50	4.5	1	0.026	591.53	0.983
70	4.5	1	0.019	427.84	0.975
100	4.5	1	0.017	352.71	0.931
100	3.0	1	0.015	199.80	0.890
100	4.5	3	0.028	111.07	0.956

where C_0 and C_t are the inlet and outlet adsorbate concentrations, respectively, z (cm) is the bed height, U_0 (cm/min) is the superficial velocity. N_0 (mg/L) is the situation concentration and K_{AB} (L/mg min) is the mass transfer coefficient. Adams-Bohart model was applied to experimental data for the description of the initial part of the breakthrough curve. This approach focused on the estimation of characteristics parameters such as maximum adsorption capacity (N_0) and the mass transfer coefficient (K_{AB}). Linear plots of ln (C_t/C_0) against time, t at different flow rates, bed heights and initial cation concentrations (Figures are not shown) were plotted. The mass transfer coefficient (K_{AB}) and saturation concentration (N_0) values were calculated from the slope and intercept of the linear curves respectively and listed in Table 5.

Although, Adams-Bohart models gives a simple and comprehensive approach for evaluating column dynamics, its validity is limited to the range of condition used. Thus the poor correlation coefficient reflects less applicability of this model [28]. The mass transfer coefficient and experimental uptake capacity along with K_{AB} and N_0 and other statistical parameters are shown in Table 5. From the Table, it is observed that, mass transfer coefficient increased with increase in bed height and flow rate but decreased with initial concentration. This showed that the overall system kinetics was dominated by external mass transfer [19, 28]. However, the sorption capacity N_0 increased for increasing initial concentration, flow rate, and bed height [24, 26, 29].

3.8. Regeneration of the Activated Carbon. It is essential to reuse the cation loaded sorbent for metal removal in industrial applications for economical feasibility of the process. Reusability of any sorbent can be determined by its adsorption performance in consecutive sorption/desorption cycles. MFSAC were tested for four cycles after the initial application, using 1 M HNO_3 as an eluting agent at flow rate of 3 mL/min for 16 hours.

Based on, Yoon-Nelson model, amount of adsorbate being adsorbed in a fixed bed column is half of total adsorbate entering within 2ζ period [21]. Thus, the sorption capacity of a column, q_{org} or q_{eq} (mg/g) is calculated from following equation and tabulated in Table 6 for each cycle:

$$\text{Capacity}, q_{eq} = \frac{C_0 r \zeta}{1000m} \tag{11}$$

Here, C_0 is the initial concentration, r is flow rate and m is mass of the activated carbon in fixed bed. However, the breakthrough time, t_b and complete exhaustion time, t_e and regeneration efficiency, according to (2) for different condition were determined and listed in Table 6.

From the tables, it can be seen that the breakthrough time is less at higher flow rate, lower bed height, and at higher inlet concentration. Experimental equilibrium uptake, q_e (mg/g) for initial concentration of 50 mg/L, 70 mg/L, and 100 mg/L solution obtained was 9.978 mg/g, 13.110 mg/g and 17.260 mg/g for batch sorption system which was higher than fixed bed system for the same concentration used. This might be due to the less effective surface area in packed bed system than the stirred batch vessels [20, 30].

4. Conclusion

This investigation showed that the granular activated carbon prepared from Mangostene fruit peel (MFSAC) was promising for removing Mn(II) ions from wastewater batch and fixed bed sorption column. The column performs better with lower feed flow rate and concentration with higher bed height. Experimental data followed Langmuir isotherm better than Freundlich at all the temperature range being studied. Column data were best-fitted with Thomas and Yoon-Nelson models. The adsorbed Mn(II) ions were desorbed quantitatively by 1 M HNO_3 and the adsorbent can be used repeatedly without significant loosing of sorption capacity reflecting its feasibility for commercial application.

Table 5: Adams-Bohart parameters for manganese(II) at different conditions using linear regression analysis.

Initial concentration (mg/L)	Bed height (cm)	Flow rate (mL/min)	K_{AB} (L/mg-min) $\times 10^{-4}$	N_0(mg/L)	R^2
50	4.5	1	2.40	488.814	0.903
70	4.5	1	1.14	529.338	0.855
100	4.5	1	0.70	700.086	0.782
100	3.0	1	0.60	698.190	0.789
100	4.5	3	1.10	762.401	0.862

Table 6: Regeneration of Column.

Metal	Cycle no.	Breakthrough time, t_b (Minute)	Column sorption capacity, q_{eq} (mg/g)	Bed exhaustion time, t_e (Minute)	Regeneration efficiency (%)
Manganese(II)	1	250	7.2573	700	original
	2	200	6.2076	630	85.53
	3	160	5.4543	450	75.15
	4	180	4.8765	280	67.19
	5	100	2.3243	220	32.03

Acknowledgments

The authors are grateful for the financial support of this project by Research Grant (UMRG 056-09SUS) of University Malaya, Kumoh National Institute, Republic of Korea (KIT), and Malaysian Agricultural Research and Development Institute (MARDI), Malaysia, for their continuous encouragement.

References

[1] I. A. Abideen, E. O. Andrew, A. I. Mopelola, and S. Kareem, "Equilibrium, kinetics and thermodynamic studies of the biosorption of Mn (II) ions from aqueous solution by raw and acid-treated corncob biomass," *Research Journal of Applied Sciences*, vol. 6, no. 5, pp. 302–309, 2011.

[2] K. L. Johnson and P. L. Younger, "Rapid manganese removal from mine waters using an aerated packed-bed bioreactor," *Journal of Environmental Quality*, vol. 34, no. 3, pp. 987–993, 2005.

[3] P. L. Sibrell, M. A. Chambers, A. L. Deaguero, T. R. Wildeman, and D. J. Reisman, "An innovative carbonate coprecipitation process for the removal of zinc and manganese from mining impacted waters," *Environmental Engineering Science*, vol. 24, no. 7, pp. 881–895, 2007.

[4] S. G. Benner, D. W. Blowes, W. D. Gould, R. B. Herbert, and C. J. Ptacek, "Geochemistry of a permeable reactive barrier for metals and acid mine drainage," *Environmental Science and Technology*, vol. 33, no. 16, pp. 2793–2799, 1999.

[5] K. A. Emmanuel and A. V. Rao, "Comparative study on adsorption of Mn(II) from aqueous solutions on various activated carbons," *E-Journal of Chemistry*, vol. 6, no. 3, pp. 693–704, 2009.

[6] Z. Z. Chowdhury, S. M. Zain, A. K. Rashid, A. A. Ahmed, M. S. Islam, and A. Arami-Niya, "Application of central composite design for preparation of Kenaf fiber based activated carbon for adsorption of manganese (II) ion," *International Journal of the Physical Sciences*, vol. 6, no. 31, pp. 7191–7202, 2011.

[7] J. N. Egila, B. E. N. Dauda, Y. A. Iyaka, and T. Jimoh, "Agricultural waste as a low cost adsorbent for heavy metal removal from wastewater," *International Journal of Physical Sciences*, vol. 6, no. 8, pp. 2152–2157, 2011.

[8] Z. Z. Chowdhury, S. M. Zain, and A. K. Rashid, "Equilibrium isotherm modeling, kinetics and thermodynamics study for removal of lead from waste water," *E-Journal of Chemistry*, vol. 8, no. 1, pp. 333–339, 2011.

[9] A. Saeed, M. W. Akhter, and M. Iqbal, "Removal and recovery of heavy metals from aqueous solution using papaya wood as a new biosorbent," *Separation and Purification Technology*, vol. 45, no. 1, pp. 25–31, 2005.

[10] M. Horsfall, A. A. Abia, and A. I. Spiff, "Kinetic studies on the adsorption of Cd^{2+}, Cu^{2+} and Zn^{2+} ions from aqueous solutions by cassava (Manihot sculenta Cranz) tuber bark waste," *Bioresource Technology*, vol. 97, no. 2, pp. 283–291, 2006.

[11] R. Aravindhan, J. R. Rao, and B. U. Nair, "Application of a chemically modified green macro alga as a biosorbent for phenol removal," *Journal of Environmental Management*, vol. 90, no. 5, pp. 1877–1883, 2009.

[12] O. S. Bello, I. A. Adeogun, J. C. Ajaelu, and E. O. Fehintola, "Adsorption of methylene blue onto activated carbon derived from periwinkle shells: kinetics and equilibrium studies," *Chemistry and Ecology*, vol. 24, no. 4, pp. 285–295, 2008.

[13] Z. Z. Chowdhury, S. M. Zain, A. K. Rashid, A. A. Ahmed, and K. Khalid, "Application of response surface methodology (RSM) for optimizing production condition for removal of Pb (II) and Cu (II) Onto kenaf production condition for removal of Pb (II) and Cu (II) Onto Kenaf," *Research Journal of Applied Sciences, Engineering and Technology*, vol. 4, no. 5, pp. 458–465, 2012.

[14] Z. Z. Chowdhury, S. M. Zain, A. K. Rashid, and M. S. Islam, "Preparation and characterizations of activated carbon from kenaf fiber for equilibrium adsorption studies of copper from wastewater," *Korean Journal of Chemical Engineering*. In press.

[15] IUPAC, *Manual of Symbols and Terminology of Colloid Surface*, Butterworths, London, UK, 1982.

[16] I. Langmuir, "The constitution and fundamental properties of solids and liquids. Part I. Solids," *The Journal of the American Chemical Society*, vol. 38, no. 11, pp. 2221–2295, 1916.

[17] H. M. F. Freundlich, "Over the adsorption in solution," *Journal of physical Chemistry*, vol. 57, pp. 385–470, 1906.

[18] M. I. Temkin and V. Pyzhev, "Kinetics of Ammonia synthesis on promoted iron catalyst," *Acta Physiochemica USSR*, vol. 12, pp. 327–356, 1940.

[19] A. A. Ahmad and B. H. Hameed, "Fixed-bed adsorption of reactive azo dye onto granular activated carbon prepared from waste," *Journal of Hazardous Materials*, vol. 175, no. 1–3, pp. 298–303, 2010.

[20] I. A. W. Tan, A. L. Ahmad, and B. H. Hameed, "Adsorption of basic dye using activated carbon prepared from oil palm shell: batch and fixed bed studies," *Desalination*, vol. 225, no. 1–3, pp. 13–28, 2008.

[21] K. S. Bharrathi, N. Badabhagni, and P. V. Nidheesh, "BREAK-THROUGH DATA ANALYSIS OF ADSORPTION OF CD (II) ON COIR PITH COLUMN," *EJEAFChe*, vol. 10, no. 8, pp. 2638–2658, 2011.

[22] G. Naja and B. Volesky, "Behavior of the mass transfer zone in a biosorption column," *Environmental Science and Technology*, vol. 40, no. 12, pp. 3996–4003, 2006.

[23] S. Mohan and G. Sreelakshmi, "Fixed bed column study for heavy metal removal using phosphate treated rice husk," *Journal of Hazardous Materials*, vol. 153, no. 1-2, pp. 75–82, 2008.

[24] H. C. Thomas, "Heterogeneous ion exchange in a flowing system," *Journal of the American Chemical Society*, vol. 66, no. 10, pp. 1664–1666, 1944.

[25] A. Ghribi and M. Chlendi, "Modeling of fixed bed adsorption: application to the adsorption of an organic dye," *Asian Journal of Textile*, vol. 1, no. 4, pp. 161–171, 2011.

[26] S. S. Baral, N. Das, T. S. Ramulu, S. K. Sahoo, S. N. Das, and G. R. Chaudhury, "Removal of Cr(VI) by thermally activated weed Salvinia cucullata in a fixed-bed column," *Journal of Hazardous Materials*, vol. 161, no. 2-3, pp. 1427–1435, 2009.

[27] Y. H. Yoon and J. H. Nelson, "Application of gas adsorption kinetics I. A theoretical model for respirator cartridge service life," *American Industrial Hygiene Association Journal*, vol. 45, no. 8, pp. 509–516, 1984.

[28] G. S. Bohart and E. Q. Adams, "Some aspects of the behavior of charcoal with respect to chlorine," *Journal of the American Chemical Society*, vol. 42, no. 3, pp. 523–544, 1920.

[29] Y. Sag and Y. Aktay, "Application of equilibrium and mass transfer models to dynamic removal of Cr(VI) ions by Chitin in packed column reactor," *Process Biochemistry*, vol. 36, no. 12, pp. 1187–1197, 2001.

[30] Z. Al-Qodah and W. Lafi, "Adsorption of reactive dyes using shale oil ash in fixed beds," *Journal of Water Supply*, vol. 52, no. 3, pp. 189–198, 2003.

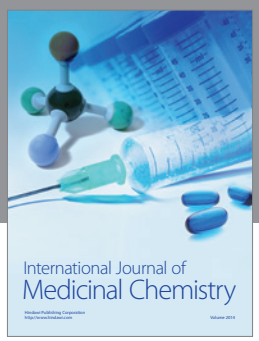

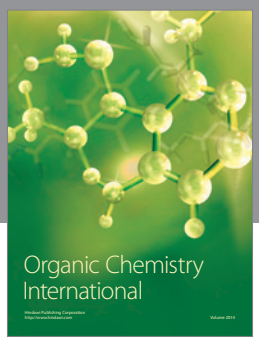

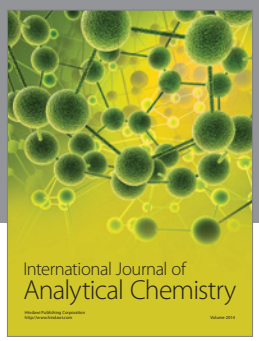

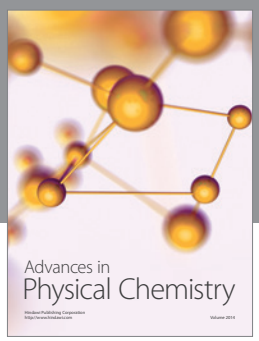

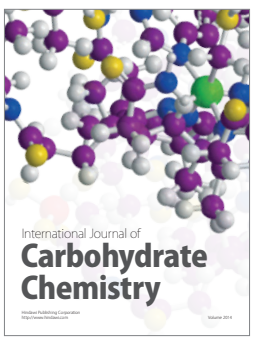

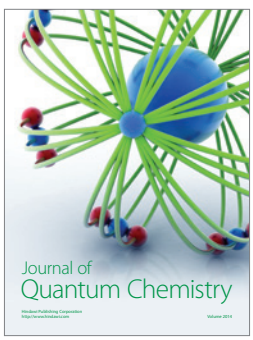

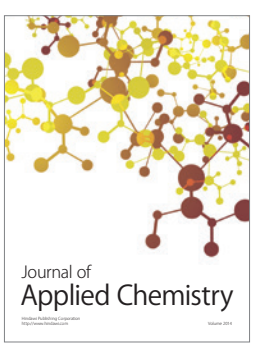

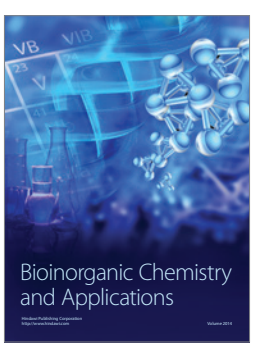

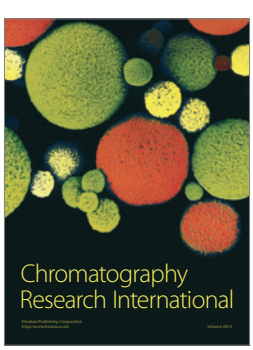

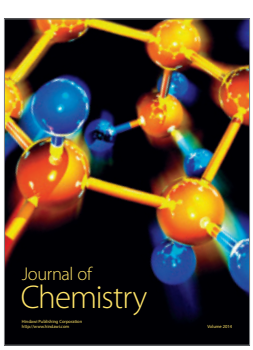

Hindawi

Submit your manuscripts at
http://www.hindawi.com